Insight into the semiconducting performance of tetraphenyldipyranylidene derivatives in organic field-effect transistors

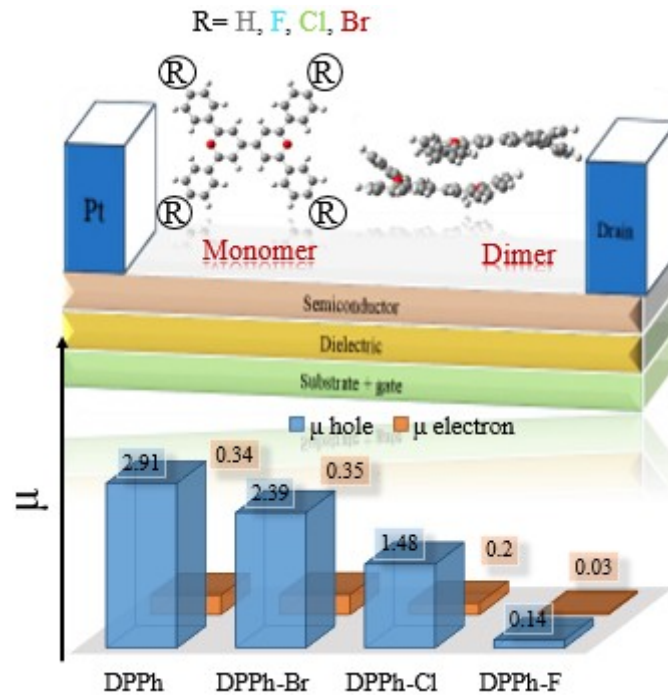**Samira Naserian, Mohammad Izadyar[*], and Foroogh Arkan**

Research Center for Modeling and Computational Sciences, Faculty of Science,

Ferdowsi University of Mashhad, Mashhad, Iran

Abstract

In this paper, Tetraphenyldipyranylidene (DPPh), a large quinoidal planar π-conjugated heterocyclic, was considered as primary organic molecule in organic field effect transistors (OFETs). Electron-withdrawing atoms such as F, Cl, and Br were attached to the H-atoms of four peripheral phenyl groups of para-positions relative to the O-atoms of DPPh. Density functional theory (DFT) calculations at the M06-2X/6-311G++ (d,p) level were performed. The influences of the different electron-withdrawing atoms such as F, Cl, and Br on the electronic and optical properties, charge transport parameters, and charge carrier mobility were investigated. The absorption and emission spectra of the DPPh and its derivatives were theoretically simulated in OFETs. The simulated spectra show an intense peak in the visible region (400-650 nm), in which the highest adsorption/emission intensity is related to DPPh-Br. Moreover, the charge injection energy barrier of DPPh and its derivatives were calculated by considering Pt as the source electrode. Based on the results, a greater hole transport is predicted than the electron transport. Moreover, the obtained ratio of the hole/electron mobility and the theoretical correlations between the charge transport parameters of monomers and dimers show that the insertion of the electron-withdrawing atoms in the DPPh structure is a promising strategy to have an ambipolar or n-type semiconductor, too. The obtained results show that introducing electron-withdrawing atoms at the para-position of the DPPh improves the hole/electron injection and transport process in the OFET devices.

Finally, DPPh-Br shows a great performance in comparison with the substituted F and Cl atoms in the OFETs devices.

1 │ INTRODUCTION

For the first time, the field-effect transistor (FET) was introduced by J. Bardeen et al in 1947.[1] In 1960, Kahng and Atalla fabricated the first silicon-based metal-oxide-semiconductor field-effect transistor (MOSFET).[2] Nowadays, MOSFET has several acronyms such as, MISFET (metal-insulator-semiconductor FET) and IGFET (insulated gate FET). New reports in this field show that the study of the stability and performance of these devices is of great interest.[3]

Organic semiconductors, such as polyaniline, were intensively investigated for industrial applications in different branches of electronics, including the photovoltaic cells (PVs),[4] light-emitting diodes (LEDs),[5] and FETs.[6] The performance of the organic semiconductors is not comparable with inorganic semiconductors due to lower electrical conductivity and short-term stability under environmental conditions.[7] But they have distinct advantages such as structural flexibility due to weak Van der Waals interactions, band gap tunability, and cheaply producing at low temperature (100–150°C).[7]

In the FETs devices, organic semiconductor layer is an important part because the transistor performance can be easily tuned by modification of this layer. Among all FETs devices, organic field effect transistors (OFETs) are more suitable alternatives than inorganic-based transistors such as amorphous silicon thin-film.[8]

Moreover, OFETs have the applied potential in smart cards, display drivers, and identification tags.[9] Also, unique properties including low-cost, simple design, small dimensions, lightweight, and flexible electronic applications make them favorable to be used in new electronic devices.[10]

Generally, an important prerequisite for semiconductor improvement is the identification of chemical and physical properties of organic semiconductors. Interestingly, organic materials (carbon-based materials) are abundant, which have no effect on reducing natural resources. In OFETs devices, the applied organic materials as semiconductor layers are classified into two types of π-

conjugated small molecules, and polymers.[11] It is well worth mentioning that small molecules in organic electronic devices have inherent advantages such as monodispersity, simple synthesis, and easier crystallization in comparison with the conjugated polymers.[12,13] In addition, the planar small molecules result in a good crystalline packing that enhances the charge carrier diffusion into material. Dipyranylidene (DP) molecule has a quinoidal structure with a C=C double bond in the para-position relative to O-atoms in the pyran heterocyclic rings (Figure 1).
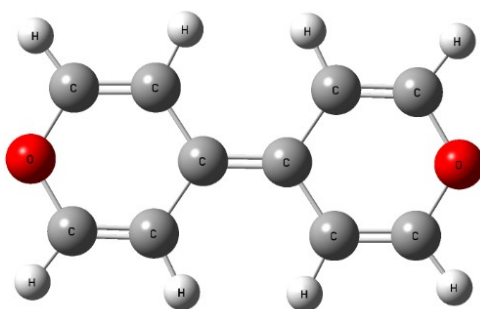

FIGURE 1 Dipyranylidene molecular structure.

2,2',6,6'-tetraphenyl-dipyranylidene (DPPh) is a type of small organic semiconductor molecule derivated from DP. In DPPh, the H-atoms of DP in the 2,2',6,6' positions relative to the O-atoms have been replaced by four phenyl groups. DPPh has an extended π-conjugation system and favorable planar structure for the strong intermolecular interactions (a good crystalline packing), enhance charge carrier mobility, and intense absorption spectrum in the UV-visible region.[9]

In 1970, the initial synthesis of DPPh was reported by Hunig et al [14] applied as an organic material in OFETs, organic bulk-heterojunction solar cells, and perovskite solar cells.[9,15,16] In 2009, it was considered as an organic semiconductor layer in OFET device by Yamashita et al.[9] They investigated the relationship between the electronic properties and chemical structure of DPPh in the FETs. Also, they analyzed the semiconducting performance of DPPh substituted by different functional groups (alkyl and halogen).

DPPh as a strong donor was combined with fullerenes in narrowband near-infrared (NIR) light detectors by Kaiser and coworkers.[17] They introduced side-chains having a stronger electron-donating strength than phenyl. [17] Based on the results, new molecules improve the efficiency of these photodetectors.

On the basis of our knowledge, the semiconducting performance of DPPh and its derivatives is unknown in electronic devices such as OFET. These compounds were considered in this work from the molecular engineering point of view. Theoretical investigations can help to provide a fundamental understanding of the substituent effect on DPPh and provide useful information for the design of high-performance organic semiconductor in OFETs devices.

Density functional theory (DFT)[18] calculations at the M06-2X/6-311G++ (d,p)[19] level were performed to study the influences of the different electron-withdrawing atoms of F, Cl, and Br on the electronic and optical properties, charge transport parameters, and charge carrier mobility. Time dependent-

density functional theory (TD-DFT)[20] calculations were used to simulate the absorption and emission spectra and finally their performances were evaluated and discussed in the OFETs.

2 │ COMPUTATIONAL DETAILS

DFT calculations are one of the prosperous theoretical approaches to investigate the correlation between the electronic and structure parameters of the molecules in the ground states (S0).[21] Moreover, TD-DFT evaluates the optical properties at the excited states (S1).[22,23]

All calculations were performed at the M06-2X/6-311++G(d,p) level of theory using the Gaussian 09 package.[24] In additions, frequency analyses were performed to ensure that the optimized structures converge to a local minimum without imaginary frequency. Also, SIESTA package[25] was used for optimization of crystal structure of DPPh at the DFT/PBE/DZP level.[26]

At the first step, the electronic and optical properties including the highest occupied molecular orbital energy (E_{HOMO}), the lowest unoccupied molecular orbital energy (E_{LUMO}), energy gaps ($E_{gap} = E_{LUMO} - E_{HOMO}$), and charge distribution on the frontier molecular orbitals (FMOs) were investigated. Furthermore, the theoretical values of absorption (λ_{abs}) and emission wavelengths (λ_{emi}), oscillator strengths (f), contribution percent (Con%), and major transitions for S0 geometries by TD-DFT calculations were evaluated. These parameters describe

various properties including charge density, charge transport, and optoelectronic nature of organic materials.

In the following, the intrinsic properties such as charge-transfer rate constant (k_{CT}), reorganization energy (λ), electronic coupling (t), ionization potential (IP), electron affinity (EA), and electron/hole extraction potential (EEP/HEP) values were calculated.

Several theoretical models, including band-like transport, hopping transport, and multiple trapping were proposed to find charge transport mechanism in organic semiconductors.[27,28] But hopping model is the most well-established model that can explain the charge transport mechanism at room temperature for organic semiconductors of OFETs.[29] According to Marcus theory,[30] the charge-transfer rate constant (k_{CT}) for the charge hopping model between two adjacent molecules is expressed by Equation (1):

$$k_{CT} = \frac{\sqrt{\pi}}{\hbar} \frac{t^2}{\sqrt{\lambda k_B T}} \exp\left(\frac{-\lambda}{4 k_B T}¿\right)¿ \qquad (1)$$

where k_B, T, and $\hbar$ are Boltzmann's constant, absolute temperature (298 K), and reduced Planck constant, respectively. Moreover, k_{CT} depends critically on two key parameters of reorganization energy (intramolecular coupling (λ)) and electronic coupling (intermolecular coupling (t)) between the adjacent molecules.

Therefore, reorganization energy shows the modification of the molecular geometry is classified to the external (λ_{ext}) and internal (λ_{int}) reorganization

energies. λ_{int} is defined as the relaxation energy of a molecule from the geometry of neutral state to the charged state (anion and cation) and vice versa. λ_{ext} is the modification in the surrounding medium as the result of polarization effects, which is negligible.[31] Therefore, the inner reorganization energy for hole (λ_+) and electron (λ_-) transfer were evaluated by using the Nelsen's four-point method (adiabatic potential-energy surface method) according to Equation (2):

[32,33]

$$\lambda = \lambda_1 + \lambda_2 \qquad (2)$$

λ_1 is defined as the difference in the single-point energy calculations of the charged molecule (x^c) at the neutral geometry (E) with geometry optimization of the charged molecules ($E^c x^c$). Also λ_2 is defined as the difference between the single-point energy calculations of the neutral molecule (x) at the charged geometry (E^c) and geometry optimization of the neutral molecule (Ex). Equations (3) and (4) are applied for this purpose, respectively.

$$\lambda_{+\, i = i\, i} \qquad (3)$$

$$\lambda_{-\, i = i\, i} \qquad (4)$$

where Ex^+/Ex^- and E^+x/E^-x are the energies of single-point cationic, anionic, and neutral molecular structures with the neutral geometry and cation/anion geometries. Also, Ex and E^+x^+/E^-x^- represent the optimization energies of neutral and cation/anion species, respectively.

Since λ shows the amount of geometrical changes upon electron/hole transfer,[34] the enhancement of λ may be attributed to the strain received from

9

structure deplanarization,[35] chemisorption induced loss of conjugation, and reducing the effective intermolecular π-orbital overlap.[36] Therefore, small λ is desirable for efficient charge transfer (electron/hole).[37,38]

Simultaneously, from four-point method[32,33] it is possible to calculate the vertical ionization potential (IP_v), adiabatic ionization potential (IP_a), vertical electronic affinity (EA_v), adiabatic electron affinity (EA_a), and electron/hole extraction potential (EEP/HEP), by using the following Equations (5-10).

$$IP_a = E^{+¿x^{+¿-Ex¿}}¿ \quad (5)$$

$$IP_v = E\,x^{+¿-Ex¿} \quad (6)$$

$$EA_a = Ex - E^{-¿x^{-¿¿}}¿ \quad (7)$$

$$EA_v = Ex - E\,x^{-¿¿} \quad (8)$$

$$HEP = E^{+¿x^{+¿-E^{¿¿}¿}}¿ \quad (9)$$

$$EEP = E^{¿}¿ \quad (10)$$

Based on the reported data on a series of the π-conjugated organic species, greater values of IP/EEP and EA/HEP lead to a favorable hole and electron transport, respectively.

Electronic coupling (t) is related to the overlap of electronic wave functions between the adjacent molecules in the solid state, which is calculated by Equation (11):

$$t = \frac{E_{L+1[H]} - E_{L[H-1]}}{2} \quad (11)$$

$E_{L+1[H]}$ and $E_{L[H-1]}$ are LUMO+1 (HOMO) and LUMO (HOMO-1) energies of the closed-shell configuration of the neutral state of the dimer for electron (hole) transfer, respectively. Theoretical calculations show that t strongly depends on the molecular packing, like π–π stacking distance and degree of π–orbital overlaps.[39]

Moreover, the intrinsic mobility of electron-hole in organic semiconductors is a key physical quantity in the charge-transport. In the zero-field, the electron/hole mobility is calculated by using the Einstein Equation (12).[40]

$$\mu = \frac{e}{k_B T} D \qquad (12)$$

where e is electronic charge and D is diffusion coefficient for n-dimensional charge transport (n=1-3) calculated by Equation (13).[41]

$$D = \frac{R^2 k}{2n} \qquad (13)$$

where R, k, and n are the effective length of the charge transfer (center-to-center distance between the molecules in the dimer), the charge transport dimensional, and the charge transfer rate constant, respectively.

Finally, the influence of different source electrode on electron/hole injection energy barrier[42] from the source electrode to organic semiconductors in the OFETs were evaluated. The electron and hole injection energy barrier (*EIE*/*HIE*) were calculated by Equations (14) and (15), respectively.

$$EIE = E_{LUMO} - \varnothing \qquad (14)$$

$$HIE = \varnothing - E_{HOMO} \qquad\qquad (15)$$

herein, ϕ is the work functions of the source electrodes[43] and both E_{LUMO} and E_{HOMO} are related to the organic semiconductors layer.

3 │ RESULTS AND DISCUSSION

3.1 │ Electronic and optical properties

Semiconductor materials are defined as an active layer for injection and transport of charge in the OFETs. In this work, DPPh was considered as the primary organic molecule and semiconductor layer in the OFET device. The effect of the substitution was investigated on the peripheral hydrogen atoms at the para-position of the phenyl rings of DPPh with electron-withdrawing groups including fluorine (F), bromide (Br), and chloride (Cl), i.e. 4'-flouro-2,2',6,6'-tetraphenyl-dipyranylidene, 4'-boromo-2,2',6,6'-tetraphenyl-dipyranylidene, and 4'-choloro-2,2',6,6'-tetraphenyl-dipyranylidene, named DPPh-F, DPPh-Br, and DPPh-Cl, respectively. The design of the organic field-effect transistor with the optimized molecular structures of DPPh and its derivatives, as organic semiconductor, is shown in Figure 2.
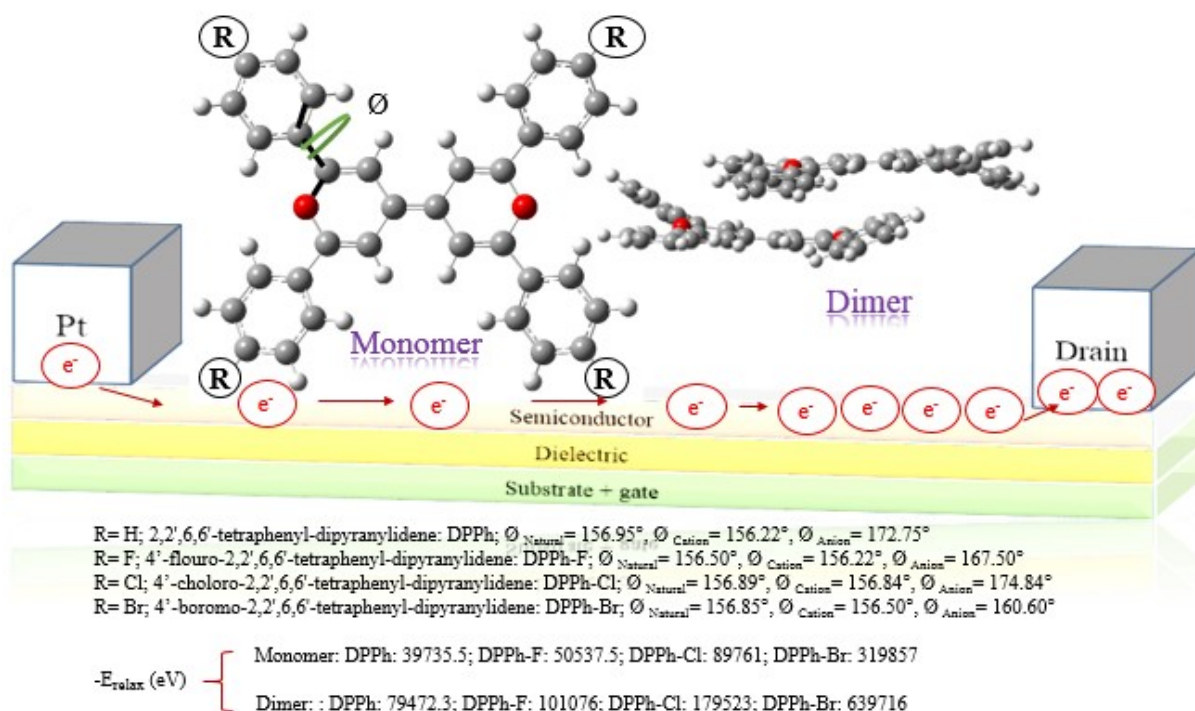
FIGURE 2 A schematic of the organic field-effect transistor along with the optimized molecular structures, dihedral angles in the neutral and ionic states, and the values of relaxed energies of dimer and monomer (-E$_{relax}$) of designed molecules calculated at the M06-2X/6-311G ++ (d, p) level.

The energies of the HOMO, LUMO, and their gap obtained and the corresponding pictorial representation is depicted in Figure 3. According to Figure 3, electron-withdrawing atoms including F and Cl increase the energies of the HOMO, LUMO, and E$_{gap}$ in comparison with DPPh, while Br substitution does not represent an important change in comparison with DPPh. Also, Figure 3 shows that electron density distribution on the HOMO is localized on dipyranylidene core for all designed molecules, in which fluorine and chlorine atoms have an important contribution. Electron density distribution on the LUMO is delocalized on whole molecule for all designed molecules.
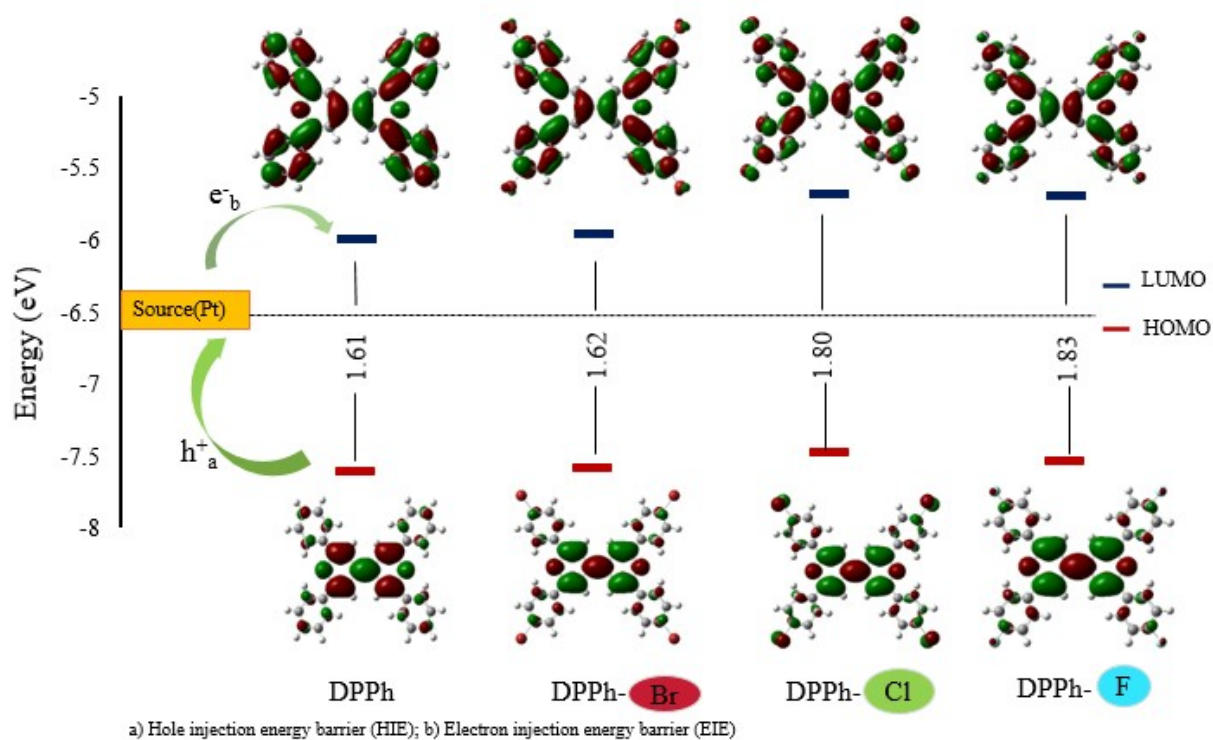
a) Hole injection energy barrier (HIE); b) Electron injection energy barrier (EIE)

FIGURE 3 The frontier molecular orbitals (HOMO→LUMO) and E_{gap} of DPPh and its derivatives calculated at the M06-2X/6-311G ++ (d, p) level.

The results of absorption/emission maximum wavelengths (see Table S1) and UV−vis absorption/emission spectrums of DPPh and its derivatives are shown in Figure 4.
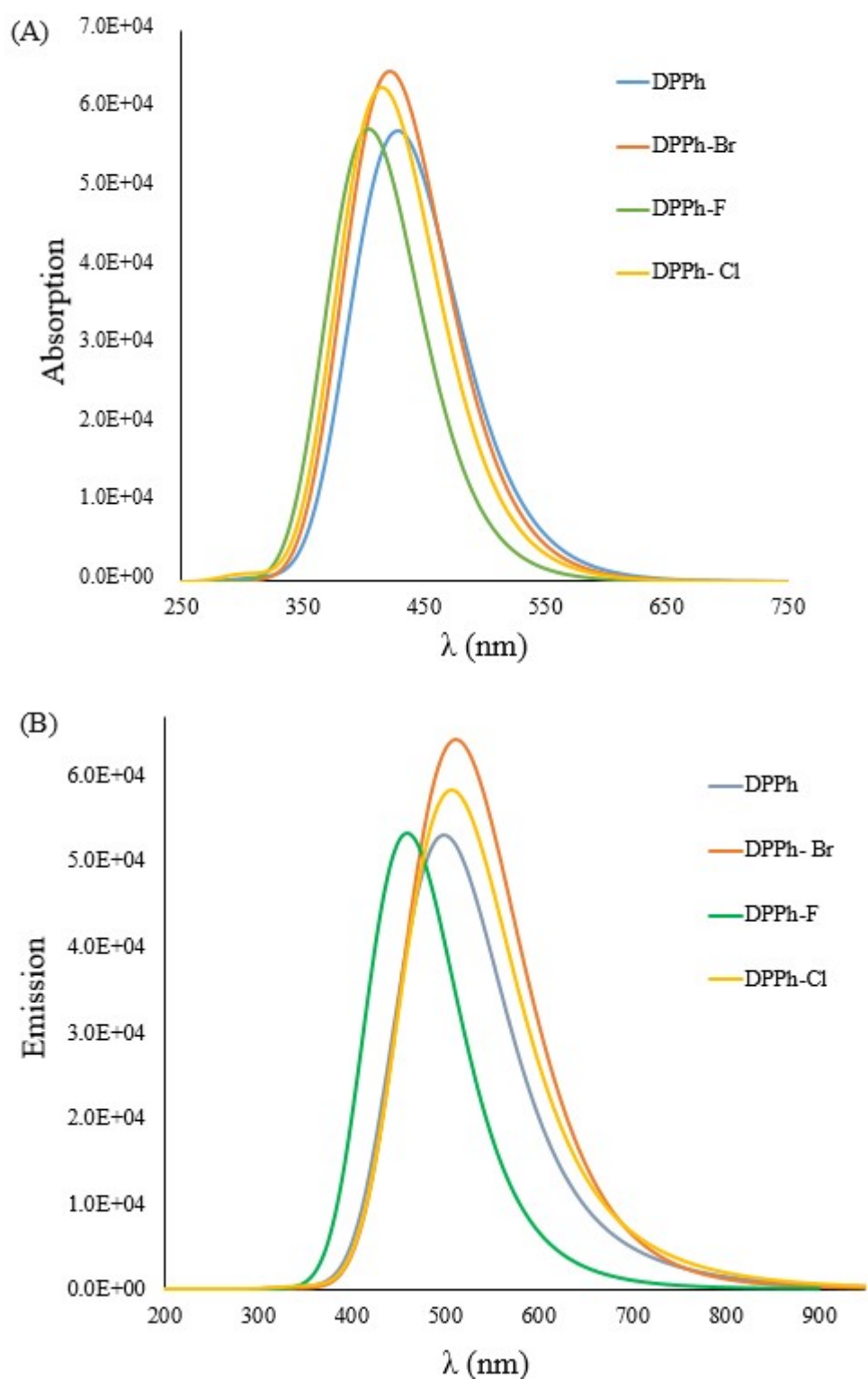
FIGURE 4 UV-visible spectra of DPPh and its derivatives, (A) absorption (B) emission

According to Table SI, the most oscillator strength and contribution percent

was observed for H → L and L→ H transitions of the absorption and emission.

Therefore, the most intense transition of $\lambda_{abs}/\lambda_{emi}$ of the designed compounds is H → L and L → H transition, respectively. The UV-visible absorption/emission spectra of the DPPh and its derivatives show an intense peak in the visible region (400-650 nm). The studied structures exhibit similar spectra in the UV−visible region with slight difference in the absorption/emission intensity. Interestingly, Table SI shows that DPPh-Br has the most oscillator strength from other studied compounds, suggesting that DPPh-Br has the highest adsorption/emission intensity (see in Figure 4).

The results of the simulated absorption/emission spectra show that these structures can be used as organic materials in photoresponsivity of organic field-effect transistors (photo-OFETs),[44] which are the basis for light sensitive transistors, e.g. light induced switches, light triggered amplification, and detection circuits. For example, photo-OFETs were operated onto MoS_2/rubrene FET[45] by light irradiation without use of source–drain bias and controlled gate bias using. The results of photo-OFETs can represent new electronic devices. Also, the studied molecules can be used as a hole transport material (HTM) in various types of electronic devices, including perovskite solar cells (PSCs), organic solar cells (OSCs), and organic light-emitting diodes (OLEDs).[15-17]

3.2 | Charge transport parameters in monomers

In the following, the hole/electron reorganization energies (λ_+/λ_-) of DPPh and its derivatives were calculated. The obtained results are shown in Table 1.

Molecules λ (eV)	DPPh	DPPh-F	DPPh-Cl	DPPh-Br
λ_+	0.41	0.44	0.43	0.42
λ_-	0.45	0.45	0.46	0.42

TABLE 1 The hole/electron reorganization energies (λ_+/λ_-) of DPPh and its derivatives calculated at the M06-2X/6-311G ++ (d, p) level.

According to Table 1, in the case of DPPh, DPPh-F, and DPPh-Cl, λ_+ is lower than λ_- that indicates that the hole transfer (p-type) is more desirable than the electron transfer (n-type). However, λ_+ increases by introducing the electron-withdrawing atoms (F and Cl) on the DPPh structure, while the hole transfer is undesirable. There is a balance between λ_+ and λ_- in DPPh-Br indicating the same ability in hole and electron transport. Therefore, it can be defined as an ambipolar-type semiconductor. Also, the dihedral angles between the phenyl rings and DP core by considering the optimized geometries of designed molecules in the natural and ionic states were represented in Figure 2. The low changes of dihedral angles for the natural molecules with the cationic state were observed in comparison with the anionic state. It can also be determined that the changes of dihedral angles for DPPh and its derivatives in the cationic state are more significant (planar) than those in the anionic state compared with the neutral state. Also, these results confirm the calculated reorganization energies

of hole of DPPh and its derivatives that are smaller than those of electron (see in Table 1).

The calculated values of IP_a, IP_v, EA_a, EA_v, EEP, and HEP of the studied molecules are represented in Table 2. The small difference in the vertical and adiabatic values of ionization potential and electron affinity demonstrated that the structural relaxation upon charge transport is small.[46] However, adiabatic energy is not often determined due to experimental work limitations, while vertical energy is easily identifiable and its values have near communicated with the experimental data. Therefore, the vertical IP and EA were considered and evaluated.

TABLE 2 Vertical/adiabatic ionization potential (IP_v/IP_a), vertical/adiabatic electron affinity (EA_v/EA_a), hole extraction potential (HEP) and electron extraction potential (EEP) of DPPh and its derivatives were calculated at M06-2X/6-311G++ (d, p) level (all values in eV).

Molecules	IP_a	IP_v	EA_a	EA_v	HEP	EEP
DPPh	5.65	5.86	0.83	0.59	5.45	1.04
DPPh-F	5.92	6.14	1.07	0.82	5.70	1.28
DPPh-Cl	5.97	6.19	1.26	1.03	5.79	1.49
DPPh-Br	6.00	6.21	1.36	1.13	5.75	1.55

According to Table 2 and, Figure 5(A) and 5(B), the theoretical trend in the EEP/IP_v and HEP/EA_v values is as follows: DPPh < DPPh-F < DPPh-Cl < DPPh-Br. A greater value of IP_v/EEP and EA_v/HEP leads to a favorable hole and electron transport, respectively. Hence, electron-withdrawing atoms have a

favorable effect on the both electron and hole transfer in DPPh. Also, the obtained values of λ_+ and λ_- decrease by the substituted F, Cl, and Br atoms (see in Table 1).
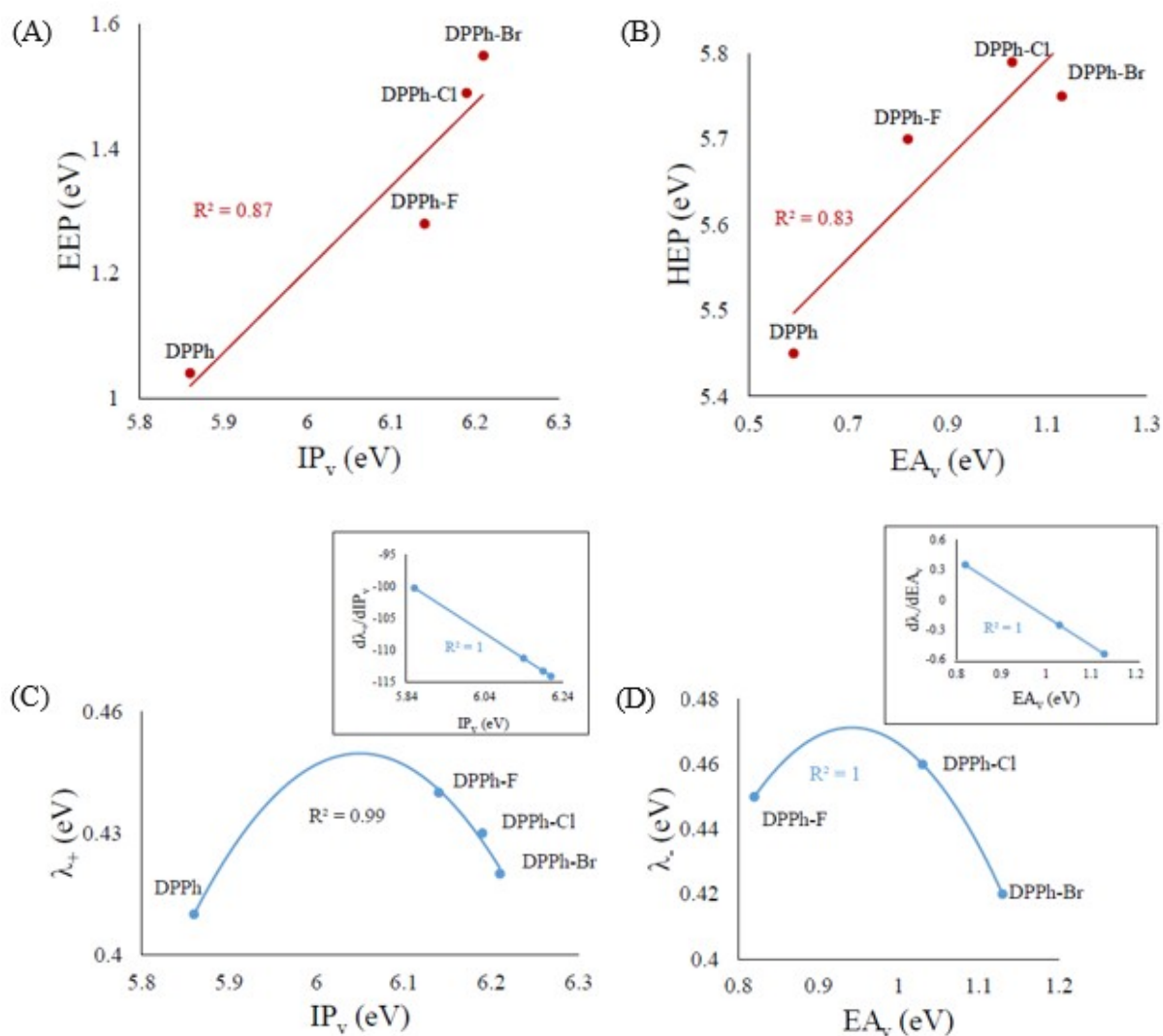

FIGURE 5 The theoretical correlation of the charge transport parameters between the studied monomers. (A) Linear correlation of the EEP and IP_v. (B) As well as HEP and EA_v. (C) The correlation of λ_+ and IP_v of the studied monomers within the differential plot of λ_+/IP_v. (D) The correlation of λ_- and EA_v of the substituted monomers within the differential plot of λ_-/EA_v.

The theoretical behaviors of λ_+ and λ_- as a functional of IP_v and EA_v of the substituted compounds by a polynomial function are shown in Figure 5(C) and 5(D), respectively. In fact, the differential plots show an increase in IP_v and EA_v values decreases the dependence of the organization energy of the hole and electron transport to IP_v and EA_v, respectively. According to the mentioned results, it can be concluded that DPPh derivatives in OFETs are favorable for the electron transfer from the p-type semiconductor to an ambipolar or n-type.

Also, the electron and hole injection energy barrier (*EIE* and *HIE* in Figure 3) of the studied monomer molecules were calculated by considering the Pt work function (ϕ= 6.38 eV)[43] and reported in Table 3.

Molecules	DPPh	DPPh-F	DPPh-Cl	DPPh-Br
EIE	0.40	0.70	0.71	0.43
HIE	1.22	1.15	1.09	1.20

TABLE 3 The theoretical values of EIE and HIE (eV) of DPPh and its derivatives at the M06-2X/6-311G ++ (d, p) level.

According to Table 3 and schematic of the HIE and EIE were depicted in Figure 2, the calculated values of EIE are lower than that of HIE, in which the substituted halides increase the electron injection energy barrier in the OFETs relative to pure DPPh. However, the values of HIE of derivatives were decreased in comparison with DPPh molecule. Therefore, the substituted

halides facilitate the hole injection greater than the considered source electrode (Pt).

3.3 | Charge transport parameters in dimers

In addition to the mentioned parameters for describing the charge transport nature and the semiconducting performance of monomer molecules in OFETs devices, the intrinsic mobility has an important role in the charge transport of dimer molecules.[47]

Packing configuration is another parameter that affects the efficient charge carrier mobility under the field-effect conditions. Based on the X-ray diffraction (XRD) analysis, there are three hopping dimers that categorized as the edge-to-face, face-to-face, and head-to-tail stacking dimers.[48,49] However, the experimental observations confirmed that the face-to-face and edge-to-face stacking geometry are more desirable than the head-to-tail configuration, because the effective $\pi-\pi$ overlap of π-stacking geometry improves the charge transport properties and charge carrier mobility.[50]

The triclinic (α-phase) and monoclinic phases (β-phase) are two polymorphs of DPPh, which are different in the growth method. A clear π-π stacking is reported for both polymorphs.[15]

The optimization of the crystal structures 2×2×2 were implemented by the conjugated gradient algorithm within the framework of the DFT with the generalized gradient approximation (GGA) in Perdew-Burke Ernzernhof (PBE), [26] the exchange-correlation functional and norm-conservative Troullier–

Martins pseudopotentials (PP),[51] and double-zeta-plus polarization function (DZP) basis set on the SIESTA package.[25,52] All atoms were fully relaxed with the cutoff energy of 220 Ry (1 eV=0.73Ry), electronic temperature of 300 K, and 1×1×1 uniform Monkhorst–Pack k-point. Figure 6 and Table S2 represent the optimized crystal structure of the α-phase and crystallographic parameters for the designed supercell structure (Figure 6(A)), respectively.   In the following, the dimer of the face-to-face π-stacking geometry of optimization of crystal structure is selected. Finally, the charge carrier mobility and charge transport properties of the selected dimer of the α-phase of the crystal structure were calculated by using the Gaussian 09 package [24] at the DFT/M06-2x/6-311G++(d,p) level (Figure 6).

According to the results of dimer and monomer molecular structures (See Figure 6(B) and 2), the relaxed energy values of monomer and dimers of DPPh and its derivatives reported in Figure 2. These values show that DPPh-Br is more stable than the primary structure and other derivatives. Also, in Figure 6(B) see that of the DPPh-Br compound has a smaller the effective distance of the charge transport than other compounds. According to these results and the results reported in Table 2, DPPh-Br can be introduced as a stable semiconductor against environmental oxidants.
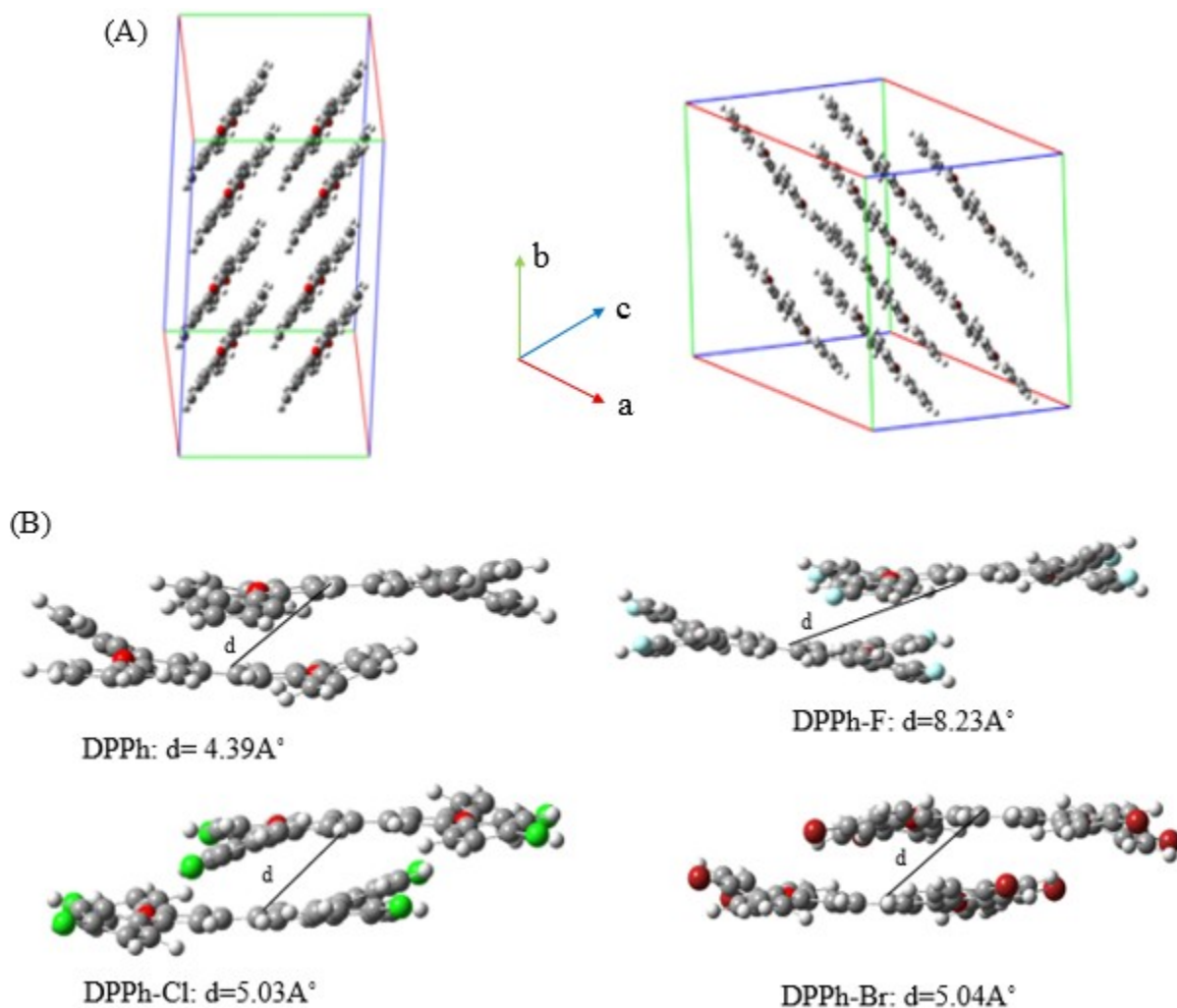
FIGURE 6 (A) The optimized crystal structure of the α-phase of DPPh (triclinic) by SIESTA at the DFT/PBE/DZP level. (B) The dimer structures of DPPh and its derivatives were optimized by Gaussian 09 at the DFT/M06-2X/6-311G++ (d,p) level (d is the effective distance of the charge transport between the monomer of dimers).

The values of transfer integral (t_+ and t_-), charge transfer rate (k_+ and k_-), charge carrier mobility (μ_+ and μ_-), hole/electron mobility ratio (μ_+/μ_-), and electron/electron mobility ratio of DPPh derivatives and designed dimers were calculated and reported in Table 4.

Dimer compounds	DPPh	DPPh-F	DPPh-Cl	DPPh-Br
$t_{+\,(eV)}$	0.08	0.01	0.06	0.07
$10^{11}k_{+\,(s^{-1})}$	30.8	0.53	15.1	24.2
$10^{-3}\mu_{+\,(cm^2.s^{-1}.V^{-1})}$	2.91	0.14	1.48	2.39
$\mu_{+\,(DPPh)}/\,\mu_{+\,(DPPh-X)}$	——	20.78	1.96	1.22
$t_{-(eV)}$	0.05	0.01	0.04	0.04
$10^{11}k_{-}(s^{-1})$	7.27	0.231	4.07	7.19
$10^{-3}\mu_{-\,(cm^2.s^{-1}V^{-1})}$	0.34	0.03	0.2	0.35
$\mu_{-\,(DPPh)}/\,\mu_{-\,(DPPh-X)}$	——	11.33	1.7	0.97
μ_{+}/μ_{-}	8.56	4.66	7.4	6.82
μ_{-}/μ_{+}	0.12	0.21	0.13	0.15

TABLE 4 The charge transport parameters (t_{+}/t_{-} and k_{+}/k_{-}), charge carrier mobility, and charge carrier mobility ratio (μ_{+}/μ_{-}) of the dimers of DPPh and its derivatives were calculated at the M06-2X/6-311G ++ (d,p) level.

According to Table 4 and Figure 7, all compounds show relatively high hole mobility, while electron mobility is lower than that of the hole. Since, the values of t_{+} are greater than t_{-} and λ_{+} are lower than λ_{-}, according to Equation (1), k_{+} becomes larger than k_{-}. Therefore, it can be concluded that higher hole mobility is related to the hole transport parameters (Table 1 and 4). Also, the obtained ratio of the hole/electron mobility confirms that hole transport is predominant to

the electron transport in the designed molecules. Moreover, the charge mobility ratio of DPPh and DPPh-Br dimers show that the hole and electron mobility of the substituted-Br compound is almost equal and slightly larger from the DPPh dimer, respectively. Moreover, the theoretical correlation between the t_+ values of the studied dimmers and the IP_v values of the studied monomers and t_- values and EA_v of the substituted compounds are depicted by polynomial and linear functions in Figure 8(A) and 8(B), respectively. The differential plot of the t_+/IP_v shows an increase in IP_v increases the dependence of hole electronic coupling to IP_v. Figure 8(B) shows that there is a linear correlation between EA_v and t_-. Hence, an increase in IP_v and EA_v values leads to a favorable hole and electron transport in dimers by considering electron-withdrawing atoms, respectively.
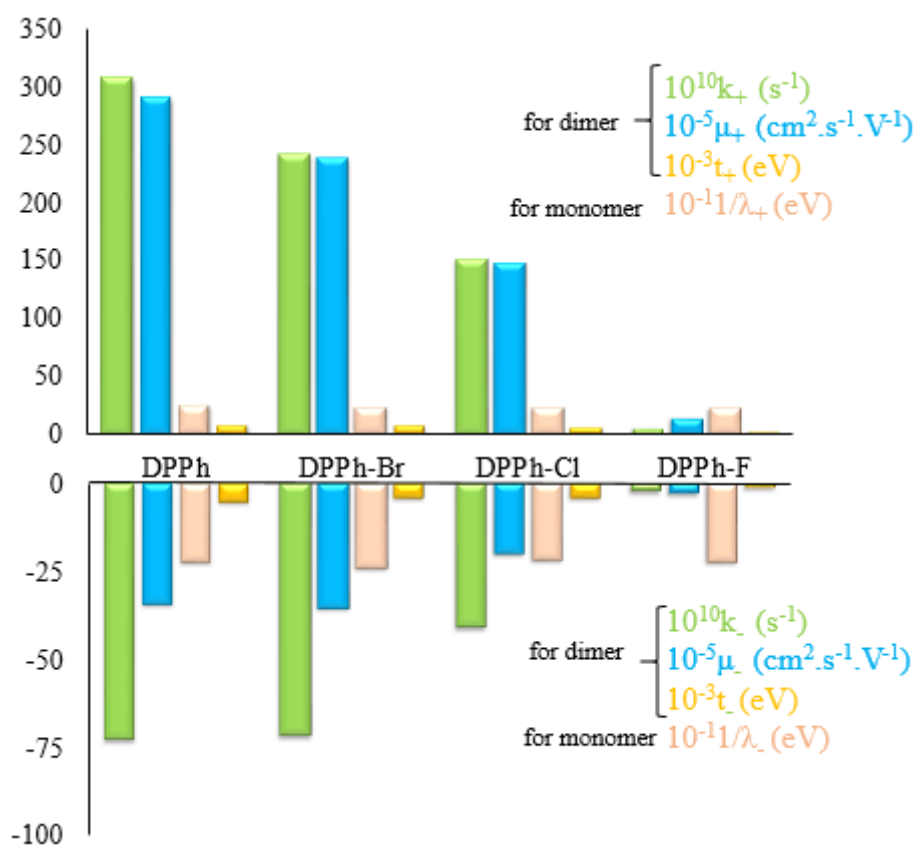
FIGURE 7 The histograms of the calculated values of charge transport parameters of k, μ, 1/λ, and t.
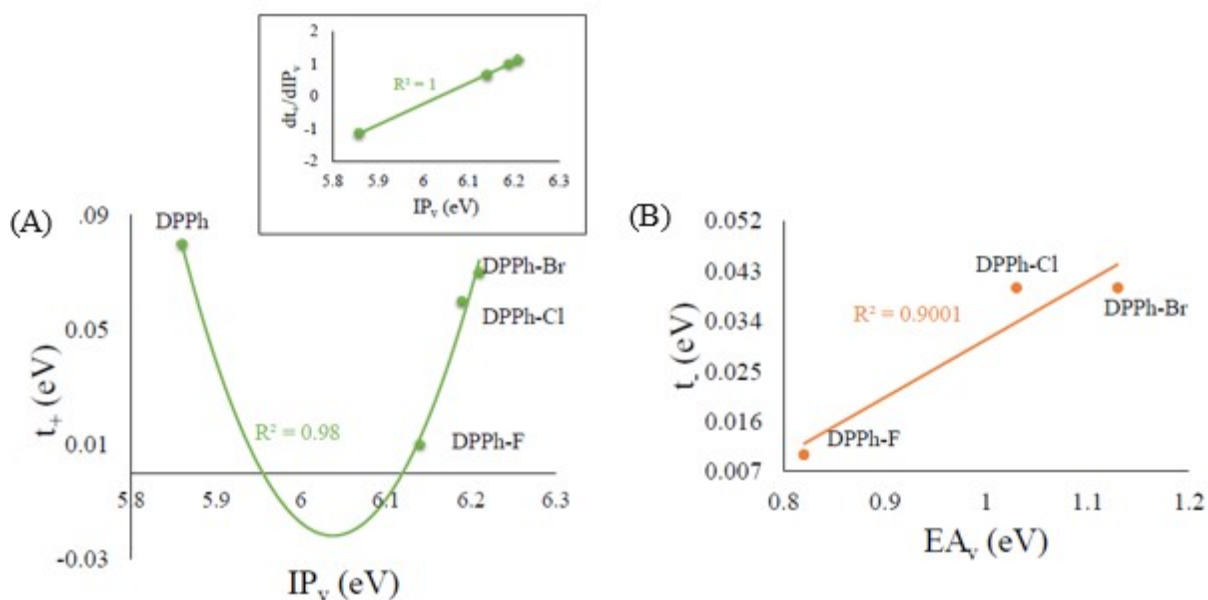

FIGURE 8 (A) The theoretical correlation of the hole electronic coupling (t_+) parameter of the studied dimers and IP_v of the studied monomers within the differential plot of t_+/IP_v. (B) The linear correlation between the electron electronic coupling (t_-) parameter of the substituted dimers and EA_v of the substituted monomers.

26

The frontier molecular orbital distribution is one of the key factors that determine the charge transport properties upon the electronic coupling of both hole and electron. In the following, the electron density distribution of the HOMO/HOMO-1 and LUMO/LUMO+1 are investigated to depict the influences of electronic coupling on the charge transfer rate and charge carrier mobility (Figure 9). Figure 9 shows that $\pi-\pi$ stacking arrangement leads to the higher electronic coupling of hole in the dimers of DPPh and DPPh-Br in comparison with both other compounds. The ratios of the hole/electron mobility (Table 4) are in correlation with the density distribution of the HOMO/HOMO-1 and LUMO/LUMO+1. Moreover, E_{gap} of the dimers and monomers are depicted in Figure 9 and 3, respectively. The results show that the HOMO and LUMO energies of the dimers shift to higher energies in comparison with the corresponding monomers. The dimers have a smaller E_{gap} than that of the monomers. These results show that the aggregated molecules have a smaller energy gap. Therefore, these results support the positive effect of Br in comparison with F and Cl atoms on DPPh. DPPH-Br can be considered as a useful semiconductor for designing high-performance organic semiconductor in OFETs devices.
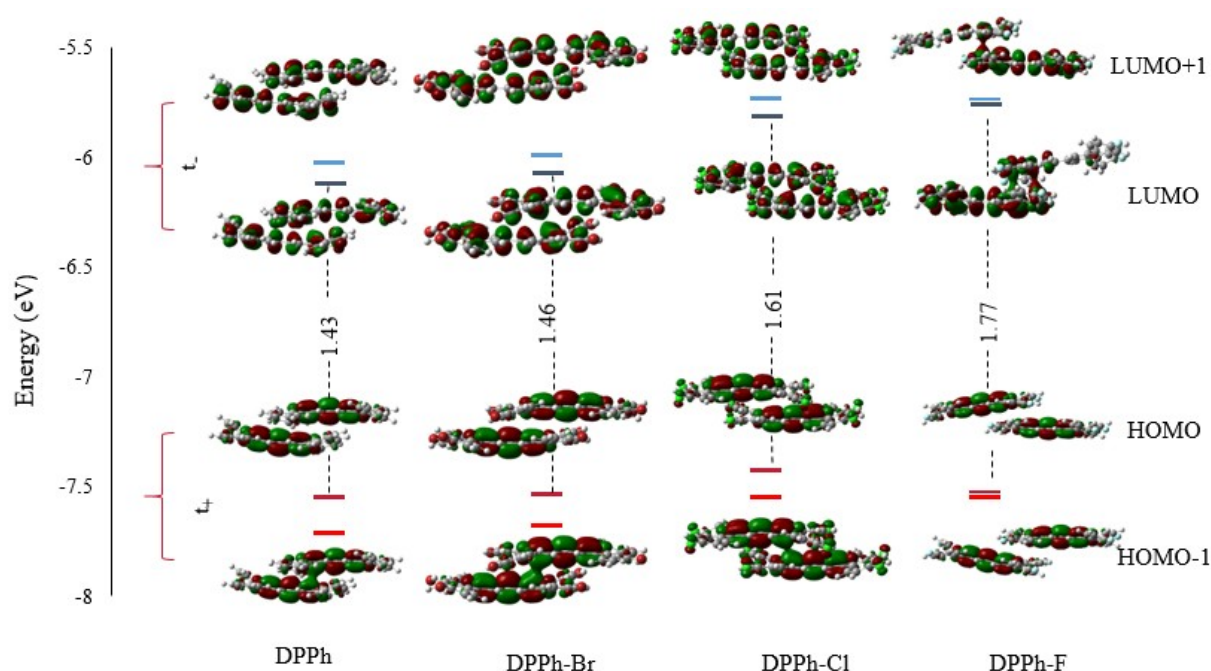
FIGURE 9 The frontier molecular orbitals electron density distribution of HOMO-1 1)/HOMO and LUMO/LUMO+1 energy levels were calculated at the M06-2X/6-311G ++ (d,p) level for the dimers of DPPh and its derivatives. Also, the values of E_{gap} of the dimer compounds were reported.

| Conclusions 4

A theoretical investigation was performed on the electronic structures, optical properties, and charge transfer parameters of DPPh and its derivatives. According to the theoretical data, the performance of these structures was analyzed in OFETs devices. The results show the high performance of the hole transfer that supports DPPh as a p-type organic semiconductor in the OFETs. The introduction of F, Cl, and Br atoms as electron-withdrawing atoms at the para- position instead of H-atoms of DPPh leads to a change in the electronic structures, optical properties, and charge transfer parameters. Br atom substitution leads to an increment in the peak intensity of the adsorption/emission spectra and greater performance than Cl and F atoms. The

charge injection barrier was calculated by considering Pt as the source electrode, which suggests that hole injection energy barrier reduces by introducing electron-withdrawing atoms, therefore, the performance of charge injection is improved in the OFETs. According to different analyses, DPPh-Br is proposed as the best candidate for hole/electron transfer, in comparison with Cl and F atoms, respectively.

REFERENCE

[1] Bardeen, J. In Great Solid State Physicists Of The 20th Century; World Scientific, **2003**, p 234-260.

[2] Kahng, D.; Atalla, M. IRE solid-state devices research conference, Carnegie Institute of Technology, Pittsburgh, PA **1960**

[3] Park, S.; Kim, S. H.; Choi, H. H.; Kang, B.; Cho, K. *Adv. Funct. Mater.* **2019**, 1904590.

[4] Bhattacharya, L.; Sharma, S.; Sahu, S. *Int J Quantum Chem* **2020**, e26524.

[5] Shirota, Y.; Kageyama, H. *Chem. Rev.* 2007, 107, 953-1010.

[6] Huang, J.; Luo, H.; Wang, L.; Guo, Y.; Zhang, W.; Chen, H.; Zhu, M.; Liu, Y.; Yu, G. *Org. Lett.* **2012**, 14, 3300-3303.

[7] Brédas, J.-L.; Beljonne, D.; Coropceanu, V.; Cornil, J. *Chem. Rev.* **2004**, 104, 4971-5004.

[8] Mallik, A.; Locklin, J.; Mannsfeld, S.; Reese, C.; Roberts, M.; Senatore, M.; Zi, H.; Bao, Z.; CRC Press, Boca Raton, FL, **2007**.

[9] Bolag, A.; Mamada, M.; Nishida, J.-i.; Yamashita, Y. *Chem. Mater.* **2009**, 21, 4350-4352.

[10] Jurchescu, O. D.; Popinciuc, M.; Van Wees, B. J.; Palstra, T. T. *Adv. Mater.* **2007**, 19, 688-692.

[11] Li, H.; Shi, W.; Song, J.; Jang, H.-J.; Dailey, J.; Yu, J.; Katz, H. E. *Chem. Rev.* **2018**, 119, 3-35.

[12] Jing, Y.; Tang, Q.; He, P.; Zhou, Z.; Shen, P. *Nanotechnology* **2015**, 26, 095201.

[13] Roncali, J.; Leriche, P.; Blanchard, P. *Adv. Mater.* 2014, 26, 3821-3838.

[14] Hünig, S.; Garner, B. J.; Ruider, G.; Schenk, W. *Justus Liebigs Annalen der Chemie* **1973**, 1973, 1036-1060.

[15] Courté, M.; Alaaeddine, M.; Barth, V.; Tortech, L.; Fichou, D. *Dyes Pigm* **2017**, 141, 487-492.

[16] Shen, C.; Courté, M.; Krishna, A.; Tang, S.; Fichou, D. *Energy Technol 2017*, 5, 1852-1858.

[17] Kaiser, C.; Schellhammer, K. S.; Benduhn, J.; Siegmund, B.; Tropiano, M.; Kublitski, J.; Spoltore, D.; Panhans, M.; Zeika, O.; Ortmann, F. *Chem. Mater.* **2019**, 31, 9325-9330.

[18] Godbout, N.; Salahub, D. R.; Andzelm, J.; Wimmer, E. *Can J Chem* **1992**, 70, 560-571.

[19] Zhao, Y.; Truhlar, D. G. *Theor Chem Acc* **2008**, 120, 215-241.

[20] Stratmann, R. E.; Scuseria, G. E.; Frisch, M. J. *J. Chem. Phys.* **1998**, 109, 8218-8224.

[21] Pedone, A. *J.Chem. Theory Comput* **2013**, 9, 4087-4096.

]22] Pedone, A.; Prampolini, G.; Monti, S.; Barone, V. *Chem. Mater.* **2011**, 23, 5016-5023.

[23] Furche, F.; Ahlrichs, R. *J. Chem. Phys.* **2002**, 117, 7433-7447.

[24] Frisch, M.; Trucks, G.; Schlegel, H.; Scuseria, G.; Robb, M.; Cheeseman, J.; Scalmani, G.; Barone, V.; Mennucci, B.; Petersson, G. Inc: Wallingford, Ct, USA **1990**, 542.

[25] Soler, J. M.; Artacho, E.; Gale, J. D.; García, A.; Junquera, J.; Ordejón, P.; Sánchez-Portal, D. *J. Phys. Condens. Matter.* **2002**, 14, 2745.

[26] Perdew, J. P.; Burke, K.; Ernzerhof, M. *Phys. Rev. Lett.* **1996**, 77, 3865.

[27] Wang, L.; Dai, J.; Song, Y. *Int J Quantum Chem* **2019**, 119, e25824.

[28] Wei, Q.; Liu, L.; Xiong, S.; Zhang, X.; Deng, W.; Zhang, X.; Jie, *J. Phys. Chem. Lett* **2019**, 11, 359-365.

[29] Wang, X.; Lau K.-C. *J. Phys. Chem. C* **2012**, 116, 22749-22758.

[30] Marcus, R. A. *Rev. Mod. Phys.* **1993**, 65, 599.

[31] Soos, Z. G.; Tsiper, E. V.; Painelli, A. *J. Lumin.* **2004**, 110, 332-341.

[32] Berlin, Y. A.; Hutchison, G. R.; Rempala, P.; Ratner, M. A.; Michl, J. *J. Phys. Chem. A* **2003**, 107, 3970-3980.

[33] Rosso, K. M.; Dupuis, M. *Theor Chem Acc* **2006**, 116, 124-136.

[34] Chen, W.-C.; Chao, I. *J. Phys. Chem. C* **2014**, 118, 20176-20183.

[35] Liu, H.; Kang, B.; Lee, J. Y. *J. Phys. Chem. C* **2013**, 117, 17832-17838.

[36] Zhang, M. X.; Zhao, G. J. *ChemSusChem* **2012**, 5, 879-887.

[37] Huang, W.; Xie, W.; Huang, H.; Zhang, H.; Liu, H. *J. Phys. Chem. Lett* **2020**, 11, 4548–4553

[38] Siddiqui, S. A.; Al−Hajry, A.; Al−Assiri, M. *Int J Quantum Chem* **2016**, 116, 339-345.

[39] Coropceanu, V.; Cornil, J.; da Silva Filho, D. A.; Olivier, Y.; Silbey, R.; Brédas, J.-L. *Chem. Rev.* **2007**, 107, 926-952.

[40] Geng, Y.; Li, H.; Wu, S.; Duan, Y.; Su, Z.; Liao, Y. *Theor Chem Acc* **2011**, 129, 247-255.

[41] TERAOKA, I.; Wiley-Interscience, Electronic, **2002**.

[42] Wang, Q.; Jiang, S.; Zhang, B.; Shin, E.-Y.; Noh, Y.-Y.; Xu, Y.; Shi, Y.; Li, Y. *J. Phy. Chem. Lett* **2020**, 11, 1466-1472.

[43] Eastman, D. *Phys. Rev. B* **1970**, 2, 1.

[44] Kanal, I. Y.; Owens, S. G.; Bechtel, J. S.; Hutchison, G. R. *J. Phys. Chem. Lett* **2013**, 4, 1613-1623.

[45] Park, C.-J.; Park, H. J.; Lee, J. Y.; Kim, J.; Lee, C.-H.; Joo, J. *ACS Appl. Mater. Interfaces* **2018**, 10, 29848-29856.

[46] Senevirathna, W.; Daddario, C. M.; Sauvé, G. v. *J. Phys. Chem. Lett* **2014**, 5, 935-941.

[47] Wang, L.; Duan, G.; Ji, Y.; Zhang, H. *J. Phys. Chem. C* **2012**, 116, 22679-22686.

[48] Letizia, J. A.; Salata, M. R.; Tribout, C. M.; Facchetti, A.; Ratner, M. A.; Marks, T. J. *J. Am. Chem. Soc.* **2008**, 130, 9679-9694.

[49] Nan, G.; Wang, L.; Yang, X.; Shuai, Z.; Zhao, Y. *J. Chem. Phys.* **2009**, 130, 024704.

[50] Winkler, M.; Houk, K. *J. Am. Chem. Soc.* **2007**, 129, 1805-1815.

[51] Troullier, N.; Martins, *J. Solid State Commun* **1990**, 74, 613-616.

[52] Sánchez−Portal, D.; Ordejon, P.; Artacho, E.; Soler, J. M. *Int J Quantum Chem* **1997**, 65, 453-461.

SUPPORTING INFORMATION

Additional supporting information may be found online in the Supporting Information section via …………...